THYROID
Volume 23, Number 7, 2013

DOI: 10.1089/thy.2012.0466

Patterns of FOXE1 Expression in Papillary Thyroid Carcinoma by Immunohistochemistry

Andrey Bychkov,[1] Vladimir Saenko,[2] Masahiro Nakashima,[3] Norisato Mitsutake,[1,4] Tatiana Rogounovitch,[1] Alyaksandr Nikitski,[1] Florence Orim,[1] and Shunichi Yamashita[1,2,5]

Background: FOXE1, a thyroid-specific transcription factor also known as TTF-2, was recently identified as a major genetic risk factor for papillary thyroid carcinoma (PTC). Its role in thyroid carcinogenesis, however, remains unknown. The purpose of the present study was to assess the relationship between the FOXE1 immunohistochemical features and the clinical and genetic characteristics of PTC.
Methods: Immunohistochemical staining of FOXE1 was performed in 48 PTC cases. Two single nucleotide polymorphisms immediately inside (rs1867277) or in the vicinity (rs965513) of the *FOXE1* gene were genotyped by direct sequencing. Histopathological, clinical, and genetic data were included in statistical analyses.
Results: FOXE1 exhibited cytoplasmic overexpression in tumor tissue compared to the normal counterpart ($p < 0.001$). Both cancer and normal thyroid cells demonstrated the highest FOXE1 scores in the areas closest to the tumor border (<300 μm) compared with more distant areas ($p < 0.001$). No differences in FOXE1 staining distributions were found between microcarcinomas and PTC of larger size, between different histopathological variants of PTC, and encapsulated and nonencapsulated tumors. Multivariate regression analysis revealed that nuclear FOXE1 expression in neoplastic cells in the vicinity of the tumor border independently associated with the genotype at rs1867277 (the dominant model of inheritance, $p = 0.037$) and tumor multifocality ($p = 0.032$), and with marginal significance with capsular invasion ($p = 0.051$).
Conclusions: FOXE1 overexpression and translocation to the cytoplasm are phenotypic hallmarks of tumor cells suggesting that FOXE1 is involved in the pathogenesis of PTC. Nuclear FOXE1 expression in tumor cells in the vicinity of the PTC border is associated with the presence of a risk allele of rs1867277 (c.-238G > A) in the 5′ untranslated region of the *FOXE1* gene, as well as with pathological characteristics of PTC, suggesting possible FOXE1 involvement in the facilitation of tumor development beginning at an early stage.

Introduction

Thyroid cancer is the most common endocrine malignancy and has shown a worldwide trend of rising incidence during the last few decades. Recently, it was reported to be among the top five leading malignancies among women in the United States (1). In Japan, the age-standardized rate of thyroid cancer increased from 1.4 in 1975 to 5.1 in 2007 (per 100,000 population) (2). Papillary thyroid carcinoma (PTC) is the major histological type and accounts for about 85% of all thyroid cancers (3).

Extensive studies in PTC have identified key molecular events of thyroid carcinogenesis including *BRAF* or *RAS* family mutations, as well as gene rearrangements (*RET/PTC*, *TRK*), which activate the MAP kinase pathway (4). In addition to advances in the understanding oncogenic changes, there has been substantial progress in the discovery of inherited genetic factors modulating the risk for PTC. Several recent genetic association studies, using genome-wide (5,6) or candidate gene approaches (7–10), concordantly revealed single nucleotide polymorphisms (SNPs) in a proximal region around (rs965513: G > A) or immediately at (rs1867277: c.-238G > A) the forkhead box E1 (*FOXE1*) gene locus as genetic markers of susceptibility to PTC in ethnically diverse populations.

The intronless *FOXE1* gene located on chromosome 9q22 encodes a DNA-binding protein also known as thyroid transcription factor 2 (TTF-2), a member of the forkhead/winged helix family of evolutionarily conserved transcription factors

Some results obtained in the course of this work were presented in part at the 54th Annual Meeting of the Japan Thyroid Association, November 21–23, 2011, in Osaka, Japan.

Departments of [1]Radiation Medical Sciences, [2]Health Risk Control, and [3]Tumor and Diagnostic Pathology; [4]Nagasaki University Research Center for Genomic Instability and Carcinogenesis; Nagasaki University Graduate School of Biomedical Sciences, Nagasaki, Japan.
[5]Fukushima Medical University, Fukushima, Japan.

(11). In humans, FOXE1 is a key player in thyroid organogenesis and thyrocyte precursor migration and differentiation, with an onset of expression in the thyroid primordium at Carnegie stage 15 (12,13). In adulthood, FOXE1 is detectible in basal keratinocytes of the epidermis, hair follicles, and in the exocrine cells of testicular seminiferous tubules (14–16). Recessive inactivating mutations in *FOXE1* are the cause of the Bamforth-Lazarus syndrome characterized by congenital hypothyroidism due to thyroid agenesis, cleft palate, choanal atresia, and spiky hairs (14). FOXE1 involvement in carcinogenesis has been demonstrated in basal and squamous cell carcinomas of the skin (16,17), breast cancer (18), and pancreatic cancer (19).

FOXE1 is a transcriptional activator of the thyroperoxidase and thyroglobulin genes (20,21). In turn, *FOXE1* expression is up-regulated in cells cultured in the presence of thyrotropin, insulin, or insulin-like growth factor-1, which are essential for thyroid follicular cell homeostasis (22).

FOXE1 involvement in thyroid diseases remains scarcely addressed. To the best of our knowledge, only a few studies have examined *FOXE1* expression at the mRNA or protein level to date. Using reverse-transcription (RT)-PCR or *in situ* hybridization, Sequeira *et al.* (23) found *FOXE1* expression in about 60% of human thyroids. In benign thyroid lesions, *FOXE1* expression was observed in 43%–100% of cases. In thyroid malignancies, *FOXE1* was expressed in 44% of follicular carcinomas, 65% of PTC, and 0 of 2 anaplastic carcinomas. Nonaka *et al.* (24) reported strong diffuse immunohistochemical FOXE1 staining in 50%–100% tumor cells in PTC, follicular adenomas, follicular carcinomas, and poorly differentiated thyroid carcinomas. Medullary thyroid carcinomas were weakly positive in 75% of the cases, and anaplastic thyroid carcinomas were virtually all negative. In a study by Zhang *et al.* (25), a gradual decrease in nuclear expression of FOXE1 was observed from follicular adenomas to anaplastic carcinomas in accordance with the degree of tumor dedifferentiation. Of note, abnormal FOXE1 expression in the cytoplasm displayed the opposite trend, except for anaplastic carcinomas, in which FOXE1 expression was generally low.

Despite genetic studies strongly implicating FOXE1 in PTC, and the observed alterations of FOXE1 expression and localization in cancer cells, its role in tumor development remains unknown. Therefore, in this study we analyzed the immunohistochemical expression patterns of FOXE1 in PTC and adjacent normal thyroid tissue in detail, and investigated their relationship with the morphological characteristics of tumors and the patients' genotypes.

Materials and Methods

Patients and tissue samples

Initially, 127 cases of PTC were collected from the archive of the Department of Tumor and Diagnostic Pathology, Nagasaki University Graduate School of Biomedical Sciences. Hematoxylin–eosin slides were reviewed to confirm the presence of neoplastic and adjacent nonneoplastic thyroid tissue large enough to assess the tumor–normal tissue interface and distant areas of both counterparts (at least 0.5 cm from the tumor border). Seventy-three cases did not match these criteria and were excluded from the study. Another six cases were excluded due to the lack of archived material for nucleic acid extraction.

Thus, a total of 48 PTC tissue samples operated on for thyroid cancer between 1977 and 2011 at the Nagasaki University Hospital were investigated. The study protocol was approved by the Ethical Committee of Nagasaki University. Clinicopathological information was retrieved from pathology records. Tumors were staged according to the UICC TNM classification of malignant tumors (26). The pathological diagnosis was based on the World Health Organization standards (27) and was confirmed independently by two pathologists (A.B. and M.N.).

Microscopic features were categorized as follows: the presence of tumor capsule (absent, partial, full; 0–2), oxyphilic changes (none, focal, moderate, severe, pure oxyphilic tumor; 0–4), multifocality (yes or no; 1–0), intraglandular spread (yes or no; 1–0), extrathyroidal extension (yes or no; 1–0), vascular invasion (yes or no; 1–0), intratumoral lymphocytic infiltration (absent, focal, severe; 0–2), peritumoral lymphocytic infiltration (absent, focal, severe; 0–2), and intratumoral fibrosis (absent, mild, moderate, extensive; 0–3). Tumor growth patterns (papillary, follicular, or solid) were scored and expressed as percentage of each component. Histologically evident concomitant thyroid diseases such as hyperplastic nodules, multinodular goiter, chronic lymphocytic thyroiditis, Hashimoto's thyroiditis, and follicular adenoma were also recorded. Patients and tumor characteristics are summarized in Table 1.

Immunohistochemical procedures

Immunohistochemistry was performed using a goat anti-human FOXE1 (ab5080, polyclonal, Abcam, Cambridge, MA) and rabbit anti-human MCM2 antibody (#3619, monoclonal, Cell Signaling, Danvers, MA). MCM2 is a member of the pre-replication complex required for the initiation of DNA replication and is widely used as a surrogate immunohistochemical marker of proliferation (28,29).

Four-micrometer-thick paraffin-embedded tissue sections were deparaffinized in xylene and rehydrated through graded alcohols. Heat-induced epitope retrieval was performed in 10 mM sodium citrate buffer (pH 6.0) using intermittent heating in four cycles of 5 minutes each in a 700 W microwave oven. Endogenous peroxidase activity was blocked by immersion in 3% H_2O_2/methanol. Ten percent rabbit serum (SAB-PO, Nichirei Biosciences, Tokyo, Japan) or 1% bovine serum albumin were used to prevent nonspecific binding for FOXE1 and MCM2 staining, respectively. Incubation with the anti-FOXE1 antibody (1:50) or anti-MCM2 (1:200) was done overnight at 4°C. The slides were subsequently incubated with Histofine Simple Stain MAX-PO(G) for FOXE1 or Histofine Simple Stain MAX-PO(MULTI) (both reagents from Nichirei Biosciences) for MCM2. Sections were visualized with diaminobenzidine, counterstained with hematoxylin, dehydrated, and mounted in permanent media.

The specificity of FOXE1 staining was validated by blocking the antibody with an excess of immunizing peptide (AYPGGIDRFVSAM; Hokkaido System Science, Sapporo, Japan). Sections were incubated with a mixture of anti-FOXE1 antibody and a gradual excess of blocking peptide overnight at 4°C followed by immunohistochemical staining as described. Negative controls (omitted primary antibody) were also stained simultaneously. A decrease in staining intensity was observed in a blocking peptide concentration-dependent

Table 1. Clinicopathological Characteristics of Cases in the Study

Age, mean ± SD (range), years	58.8 ± 9.7 (40–76)
Sex	
Male	5 (10.4%)
Female	43 (89.6%)
pT category[a]	
1	19 (39.6%)
2	7 (14.6%)
3	20 (41.7%)
4	2 (4.2%)
N1 category[a]	27 (56.3%)
M1 category[a]	0 (0.0%)
Clinical stage	
I	15 (31.3%)
II	3 (6.2%)
III	28 (58.3%)
IV	2 (4.2%)
Tumor size, mean ± SD (range), mm	18.9 ± 8.6 (5–45)
≤ 10 mm	8 (16.7%)
11–20 mm	28 (58.3%)
> 20 mm	12 (25.0%)
Tumor capsule (full/partial)	12 (25.0%)
Capsular invasion	8 (16.7%)
Histopathological variant	
Papillary	28 (58.3%)
Follicular	5 (10.4%)
Other[b]	15 (31.2%)
Oxyphilic changes[c]	18 (37.5%)
Tumor multifocality	7 (14.6%)
Intrathyroidal spread	26 (54.2%)
Extrathyroidal extension	20 (41.7%)
Vascular invasion	19 (39.6%)
Intratumoral lymphocytic infiltration	11 (22.9%)
Peritumoral lymphocytic infiltration	36 (75.0%)
Tumor fibrosis[d]	31 (64.6%)
Concomitant thyroid disease[e]	16 (33.3%)

Values are *n* (%) unless otherwise noted.
[a]pT (pathologically assessed primary tumor size and extension), N (regional lymph node involvement), and M (distant metastasis) categories are defined according to UICC TNM classification (26).
[b]Solid variant, oxyphilic variant and tumors with mixed growth pattern.
[c]Includes focal oxyphilic changes and oxyphilic tumors.
[d]Only moderate/extensive fibrosis.
[e]Includes solitary hyperplastic nodules, multinodular goiter, chronic lymphocytic thyroiditis, Hashimoto's thyroiditis, and follicular adenomas.

manner (Supplementary Fig. S1; Supplementary Data are available online at www.liebertpub.com/thy). No staining was seen in negative controls.

Immunohistochemical scores

The evaluation of the FOXE1 score and MCM2 labeling index was performed by observers blinded to clinical, demographic, and genetic data. The intensity of immunoreactivity was classified as negative (0), mild (1), intermediate (2), or strong (3). The proportion score was semiquantitative and comprised the percentage of stained tumor cells ranging from 0% to 100% in 5% increments (0%, 5%, 10%, etc.). The resultant score was calculated by multiplying staining intensity by the proportion score.

FOXE1 scores were calculated separately for nuclear and cytoplasmic compartments. Based on the preliminary observations, four distinct zones in each section were distinguished. These were the tumor (T) and normal (N) counterparts both subdivided into the close and distant areas with regard to the proximity to the border between cancer tissue and adjacent normal thyroid tissue. T close and N close were defined as areas of parenchyma extending up to 300 μm from the tumor border for both cancerous and nonneoplastic thyroid. Correspondingly, T distant and N distant were the areas outside (>300 μm) the close ones. The FOXE1 score was evaluated at ×400 magnification throughout each zone in cell nuclei and cytoplasm separately. The total FOXE1 score is reported as the sum of nuclear and cytoplasmic scores in cancer or normal tissues across all the zones. At least 1000 cells were counted in four random fields of each zone.

MCM2 index was calculated as a percentage of positive cells (nuclear staining regardless of intensity) among at least 1000 tumor cells counted in four random fields in the T close and T distant zones. Nonepithelial cells (e.g., lymphocytes) were ignored.

SNP genotyping

Tissues were manually microdissected from three 4 μm formalin-fixed paraffin-embedded sections and DNA was extracted using RecoverAll Total Nucleic Acid Isolation Kit (Ambion, Applied Biosystems, Foster City, CA) according to the manufacturer's instructions. DNA quantification was performed using a NanoDrop 1000 spectrophotometer (Thermo Fisher Scientific, Waltham, MA). SNPs (rs965513 and rs1867277) were detected by direct sequencing. Primers were designed with Primer Express Software Version 1.0 (Applied Biosystems) to yield relatively short PCR products (around 100 bp) suitable for sequencing with the forward primer. Primer sequences were as follows: 5′-AAT GTA GGT TTT TGG TGA TGG TAT GG-3′ (rs965513F), 5′-GTG AGA ACA GAC TAA TAC ATC TTC TTT TTA ATT T-3′ (rs965513R), 5′-ACC CCA ACC CAG GGA TCA-3′ (rs1867277F), and 5′-AGC GGC GGT GGC CTC-3′ (rs1867277R). PCR amplifications were routinely performed for 35 cycles in a final volume of 25 μL with the TaKaRa ExTaq Hot Start Version enzyme (Takara, Shizuoka, Japan) and 50–100 ng of DNA template. A single band of PCR product of expected molecular weight was confirmed on a 2% TAE agarose gel. Amplified products were treated with ExoSAP-IT cleanup reagent (Affymetrix, Santa Clara, CA) and sequenced with the BigDye Terminator v3.1 Cycle Sequencing Kit (Applied Biosystems) on an ABI PRISM 3130xl Genetic Analyzer (Applied Biosystems).

Statistical analysis

FOXE1 is a transcription factor whose principal functions are expected to be in the nucleus. Thus, all cases in the study were dichotomized according to the nuclear immunohistochemical FOXE1 scores in either the T close or N close zones into (i) cases with scores below or (ii) equal to or greater than median. These defined subgroups were compared for baseline factors and clinical and tumor-related characteristics by Fisher's exact test or its extension (http://in-silico.net/tools/statistics/fisher_exact_test) for categorical data and the Mann-Whitney test for continuous variables with the SPSS 17.0 statistical software package (SPSS, Chicago, IL).

For multivariate analysis, the following variables were tested: age (continuous, years), sex (categorical, male or

female), tumor size (continuous, mm), nodal disease (categorical, yes or no), presence of tumor capsule (categorical, yes or no; the category yes including both partially and fully encapsulated tumors), tumor growth pattern (categorical; based on histological subtypes or their combinations in the tumor tissue: papillary, follicular or other; the category other included the solid variant and tumors with mixed growth pattern), oxyphilic changes (categorical; yes or no; the category yes included focal, moderate, severe oxyphilic changes and pure oxyphilic tumors), multifocality (categorical; yes or no), intraglandular spread (categorical; yes or no), extrathyroidal extension (categorical; yes or no), vascular invasion (categorical; yes or no), intratumoral lymphocytic infiltration (categorical; yes or no; the category yes included both focal and severe infiltration), peritumoral lymphocytic infiltration (categorical; yes or no; the category yes included both focal and severe infiltration), intratumoral fibrosis (categorical; yes or no; the category yes included moderate and extensive fibrotic changes), concomitant thyroid disease (categorical; yes or no), rs965513 and rs1867277 SNPs (both ordinal; the dominant inheritance model which combined cases heterozygous and homozygous for the minor allele vs. homozygous wild-type was used), and the MCM2 labeling index (ordinal, index below vs. equal to or greater than median). Nonautomatic backward elimination was applied to the full model that included all the variables listed above. Once the most appropriate model was determined, the maximum likelihood estimates of the respective parameters and their 95% confidence intervals were calculated.

For linkage disequilibrium analysis, the CubeX web tool was used (www.oege.org/software/cubex).

A p-value of < 0.05 was regarded as indicating statistical significance in all tests.

Results

Immunohistochemical FOXE1 staining

Normal thyroid follicular cells exhibited nuclear and cytoplasmic FOXE1 staining. Nuclear immunoreactivity was strong or moderate with solid appearance, while the cytoplasm displayed a focal granular staining of weak intensity. Approximately one third of all nuclei were FOXE1 negative, whereas no cytoplasmic expression was noticed in about 25% of cells (Supplementary Fig. S2a). A more uniform pattern of FOXE1 expression was observed in cells in the vicinity of the tumor border confined within the $\leq 300\ \mu$m tissue layer (Fig. 1a and 1b). In all cases most cells showed strong nuclear and moderate cytoplasmic (predominantly along the luminal membrane) immunoreactivity (Supplementary Fig. S2b).

In tumors, FOXE1 expression was moderate to strong, thus the neoplastic area was easily distinguishable from adjacent normal parenchyma on low-power microscopy (Fig. 1b). Cytoplasmic immunoreactivity was observed in all cancer cells regardless of their spatial localization. Nuclear expression often had a rim-like appearance reflecting chromatin distribution in PTC nuclei (Fig. 1e). Similarly to the normal thyroid, FOXE1 expression in the cells at or in close proximity to the tumor border showed the highest intensity of cytoplasmic and nuclear expression (Supplementary Fig. S2c). Neoplastic cells in the tumor center exhibited markedly lower intensity often accompanied by the loss of nuclear expression (Supplementary Fig. S2d). Cancer cells embedded in fibrous tissue displayed increased immunoreactivity, while in contrast FOXE1 expression in the areas with oxyphilic changes was low.

FOXE1 expression patterns in PTC

The total FOXE1 score (combining close and distant zones) was significantly higher in cancer tissue as compared to normal thyroid ($p < 0.001$; Fig. 2). This was mostly due to the higher cytoplasmic FOXE1 expression in cancer cells ($p < 0.001$). In contrast, nuclear expression was higher in nonneoplastic thyroid than in tumor tissue, although with borderline significance ($p = 0.048$). Cytoplasmic FOXE1 expression was an essential feature of cancer cells, while prominent nuclear expression was characteristic for normal cells. Of note, all cancer cells, but not all normal cells were immunopositive for FOXE1.

Statistical analysis confirmed our preliminary observations of a gradient in FOXE1 expression between central and peripheral areas of tumor and normal tissues (Supplementary Fig. S2a–d, Fig. 2). Both cancer and surrounding normal thyroid tissues concordantly demonstrated the strongest FOXE1 staining in the areas immediately adjacent to the tumor border as compared with that in distant regions ($p < 0.001$). The highest nuclear scores were in the normal tissue; conversely, the highest cytoplasmic scores were observed in the tumors. There were pronounced changes in FOXE1 immunoreactivity with distance from the tumor border such as an increasing number of negative nuclei in the normal thyroid tissue, and a decreasing cytoplasmic intensity with increasing number of negative nuclei in cancer tissue.

Taking into account the differences in FOXE1 scores between neoplastic and nonneoplastic thyroid and the gradient between proximal and distant (relative to the tumor border) areas, we distinguished four distinct patterns of FOXE1 expression:

1. In the N distant zone (nonneoplastic thyroid tissue outside the N close zone, i.e., $>300\ \mu$m from the tumor border) there was a considerable variation of nuclear and cytoplasmic FOXE1 expression with 25%–35% FOXE1-negative cells (Fig. 1c, Supplementary Fig. S2a).
2. In the N close zone (normal thyroid tissue immediately adjacent to invasive or encapsulated tumor border, i.e. $\leq 300\ \mu$m) most cells were FOXE1-positive and showed the highest nuclear and moderate cytoplasmic intensity (Fig. 1d, Supplementary Fig. S2b).
3. In the T close zone (invasive tumor front or subcapsular region within $300\ \mu$m, regardless of the tumor border being in contact with adjacent thyroid parenchyma or extrathyroidal tissues) virtually all cells demonstrated the strongest cytoplasmic and moderate nuclear FOXE1 expression (Fig. 1e, Supplementary Fig. S2c). The presence or absence of a capsule as well as its thickness did not affect the size of the zone.
4. The T distant zone (bulk PTC tissue at a distance of $>300\ \mu$m from the border) shows mainly monomorphic low to moderate cytoplasmic expression with negative or weak nuclear staining (Fig. 1f, Supplementary Fig. S2d).

The cytoplasmic and nuclear FOXE1 scores in both tumor and normal tissue moderately, but significantly correlated with each other in all four zones ($p < 0.002$ for any

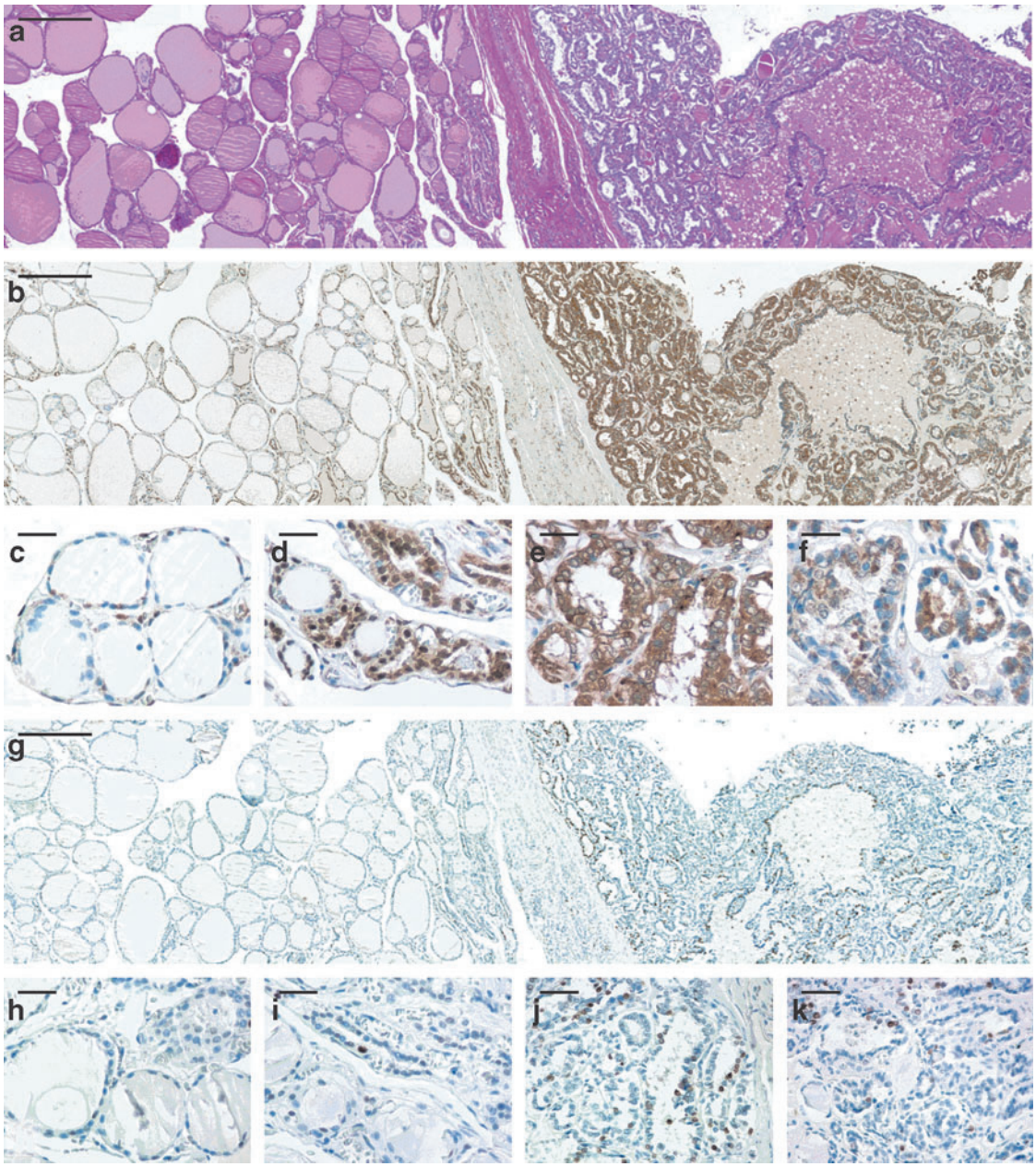

FIG. 1. Expression patterns of FOXE1 and MCM2 in papillary thyroid carcinoma (PTC) and adjacent nonneoplastic thyroid. **(a)** Low-power view of encapsulated PTC and surrounding thyroid tissues stained with hematoxylin and eosin. **(b)** Immunohistochemical FOXE1 staining demonstrates the highest expression at the tumor/normal tissue interface in both counterparts. **(c–f)** High-power fields of FOXE1 expression in the N distant, N close, T close, and T distant zones, respectively. **(g)** Panoramic view of MCM2 immunostaining in PTC showing prominent labeling of cancer tissue as compared to the very low index in the normal counterpart. **(h–k)** High-power fields of MCM2 expression in the N distant, N close, T close, and T distant zones, respectively. Serial sections, scale bars 300 μm **(a, b, g)** and 30 μm **(c–f, h–k)**.

relationship; R^2 range, 0.19–0.52). However, there was no correlation between any FOXE1 scores in each zone when normal and cancer tissues were compared pairwise ($p > 0.07$ for any relationship).

Of note, papillary microcarcinomas showed the same pattern as large-sized tumors ($p > 0.34$ for difference in any FOXE1 score). Moreover, no significant variations in FOXE1 expression patterns were found between histological variants of PTC ($p > 0.27$ for difference in any FOXE1 score).

MCM2 expression by immunohistochemistry

To address whether FOXE1 distribution patterns could be associated with proliferation, MCM2 staining was employed. A diffuse nuclear immunostaining was observed across neoplastic tissue (Fig. 1g). There was marked intertumor variation of the labeling index ranging from 0.96 to 54.58 (24.88, mean). In most PTCs, MCM2 expression was higher in the invasive zone than in the central area (Fig. 1j, k), 29.6 ± 14.4 vs. 20.16 ± 12.5 ($p = 0.003$). However, tumors measuring ≤ 1 cm

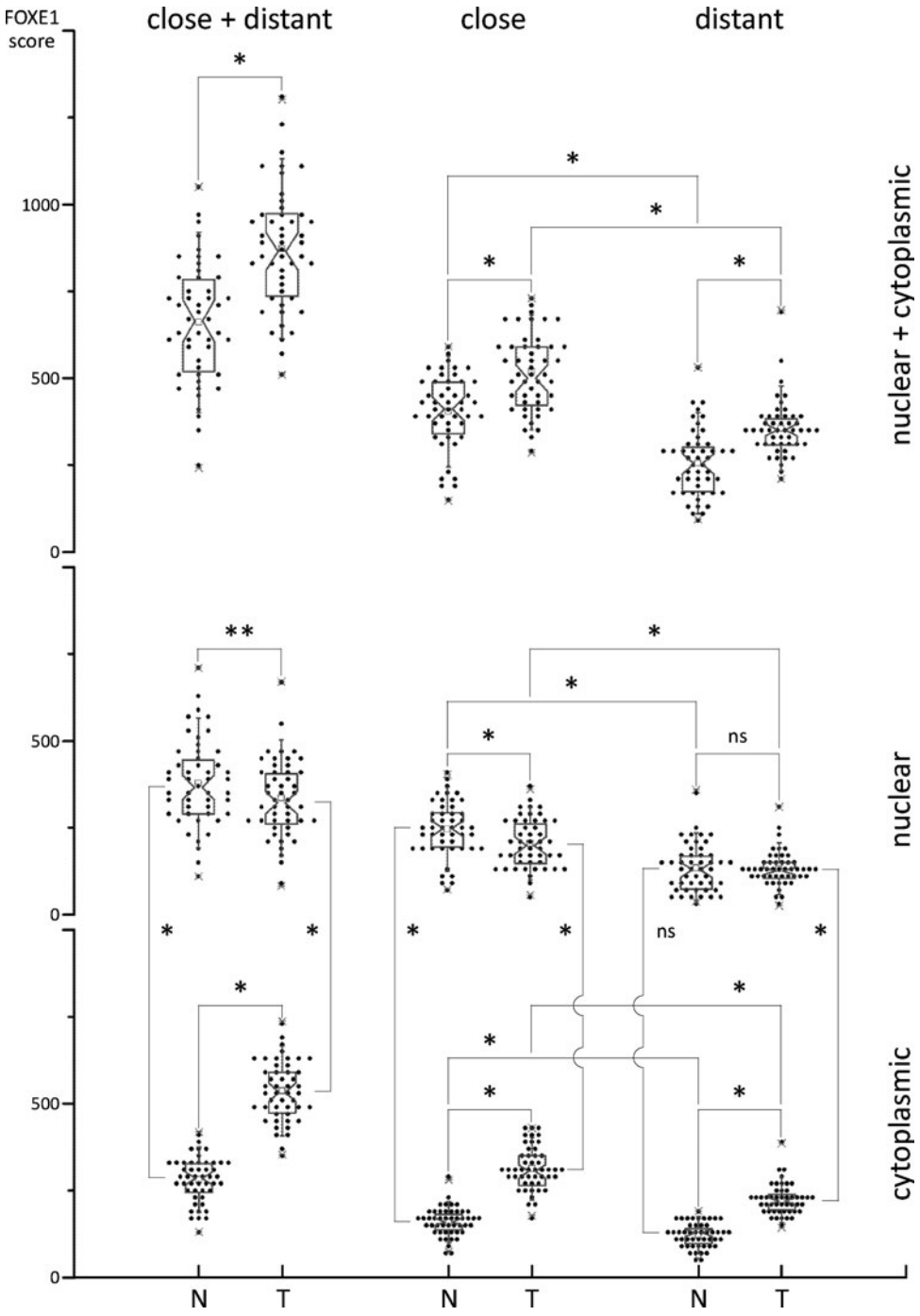

FIG. 2. FOXE1 immunoreactivity scores in PTC and adjacent normal thyroid tissue. Box-and-whisker/dot plots showing the distributions of cytoplasmic and nuclear FOXE1 scores in the close and distant zones of normal thyroid (N) and tumor tissue (T). The bottom and top lines of the box represent the values corresponding to the 25th and the 75th percentiles, respectively; position of the notch represents the median; a small inner square indicates the mean; the range represented by the whiskers corresponds to the 10th and the 90th percentiles; the crosses correspond to the 1st and the 99th percentiles. Differences between the scores were evaluated using the Mann-Whitney *U*-test: $*p < 0.01$; $**p < 0.05$; ns, nonsignificant.

(*i.e.*, microcarcinomas) failed to display this pattern, 29.4 ± 14.6 vs. 24.3 ± 14.3 ($p = 0.672$). Cancer epithelial cells in the areas of lymphocytic infiltration were often strongly positive for MCM2. Furthermore, PTCs with severe intratumoral lymphocytic infiltration showed a significantly higher MCM2 index ($p = 0.021$). In addition, PTCs displaying oxyphilic changes demonstrated an elevated labeling index, 35.7 ± 12.2 vs. 25.2 ± 14.5 ($p = 0.016$). The MCM2 index correlated with total and nuclear FOXE1 scores in both close and distant neoplastic zones ($p < 0.05$ for any comparison), but not with the cytoplasmic FOXE1 score ($p > 0.17$ for any comparison).

In the normal thyroid, MCM2 expression was exceedingly low. While normal follicular epithelium immediately adjacent to the tumor showed a slightly higher MCM2 score than that at the greater distance, the number of positive cells accounted for less than 1% (Fig. 1h–i). MCM2 labeling indices in the normal thyroid did not correlate with any of the corresponding FOXE1 scores.

Based on the difference in FOXE1–MCM2 correlations between normal thyroid and cancer tissue we concluded that FOXE1 expression is not specifically associated with cell proliferation.

Genetic analysis of FOXE1 *polymorphism*

Two SNPs in the *FOXE1* locus have been reported to significantly associate with thyroid cancer risk. The strongest marker, rs965513 (G > A) (5,6,8,9), lies about 57 kb upstream (centromeric) to *FOXE1* and a functional variant rs1867277 (G > A) is located within the *FOXE1* 5′ untranslated region (UTR) (c.-238) (7). The two SNPs were successfully genotyped in 47 and 46 cases, respectively. In agreement with our previous independent study (8) and dbSNP build 137 (www.ncbi.nlm.nih.gov/sites/entrez?db=snp), rs965513 had a minor allele frequency of 0.053 (0.057 in the Japanese population in both references) and rs1867277 of 0.170 (0.172 and 0.108 according to the two references, respectively). There was no strong evidence for linkage disequilibrium between the two SNPs in the present series ($D' = 0.21$) in line with our earlier findings ($D' = 0.23$) (8).

Association of immunohistochemical FOXE1 expression with clinicopathological and genetic parameters

Nuclear FOXE1 expression in the T close and N close zones were chosen as the outcome variables.

As shown in Table 2, on univariate analysis of the T close zone, none of the parameters was significant, except MCM2 immunohistochemical expression in the distant zone of the tumor as mentioned above. Nuclear FOXE1 expression in the N close zone associated with only two parameters, the intratumoral lymphocytic infiltration and MCM2 immunohistochemical expression in the distant zone of the tumor.

The results of multivariate logistic regression analysis demonstrated that among all variables tested only two, the multifocality ($p = 0.032$) and rs1867277 polymorphism in the *FOXE1* 5′ UTR ($p = 0.037$), significantly associated with nuclear FOXE1 expression in the T close zone; capsular invasion displayed marginal significance ($p = 0.051$) as shown in Table 3. Both multifocality and variant genotype other than homozygous for the major allele (the dominant model of inheritance) were associated with higher FOXE1 expression. In contrast, the regression models for the N close zone performed poorly, and no variables significantly associating with nuclear FOXE1 expression in this zone could be identified.

Discussion

Our study reports, for the first time, FOXE1 expression decreasing with distance from the tumor border in both PTC neoplastic and adjacent normal thyroid tissue, FOXE1 overexpression in cancer cells accompanied by a prominent translocation to the cytoplasm, and the association of nuclear FOXE1 level in cancer cells with a SNP in the 5′UTR of the gene.

The interface between normal and cancer tissue is characterized by the highest intensity of several biological processes including cell metabolism, proliferation, neovascularization, and invasion. Gradient staining intensities between peripheral and central parts of the tumor have been shown for proliferative markers Ki-67 and MCM-2 in follicular thyroid carcinomas (30,31), nuclear β-catenin in colorectal cancer (32,33), tumor-specific C-reactive protein in renal cell carcinomas (34), MMP-2 and MMP-7 in colorectal adenocarcinomas (35), and VEGF-A in astrocytomas (36). Not only cancer epithelial cells but also stromal components, primarily the immune cells, may display distance-dependent distribution from tumor periphery to central areas. For example, lymphocytes and dendritic cells tend to infiltrate the periphery of PTC rather than the intratumoral region (37,38). Tumor-associated macrophages are also localized predominantly in the peripheral areas of the follicular variant of PTC (39). Our observation of differences in FOXE1 expression between PTC periphery and tumor center is generally in line with the increased cellular activity at the tumor border.

However, a similar gradient was also detected in non-neoplastic thyroid tissue adjacent to PTC. This form of distribution has not been sufficiently described for the normal counterpart. Tumor cells can directly influence surrounding host tissue, but this is mostly known to affect peritumoral stroma, which undergoes changes resembling some properties of cancerous stroma (40). It is unlikely that physical contact between cancer and normal cells at the tumor border is the reason for local FOXE1 overexpression, since there was no obvious difference in expression patterns between encapsulated and nonencapsulated tumors. Moreover, there was no relationship with capsule thickness or tumor size. It is conceivable that FOXE1 overexpression may be due to humoral factors secreted by cancer or normal cells, either epithelial or stromal, but this hypothesis requires further investigation. The fact that nuclear FOXE1 expression in normal thyroid tissue in the vicinity of the tumor border was not associated in multivariate analysis with any tumor characteristic hampers assumptions about the significance of such an accumulation. It could be a reactive change, but whether it provides a positive or negative feedback to the tumor remains to be established.

In order to explain FOXE1 overexpression around the tumor border, we explored several markers. We observed that the MCM2 index decreased with increasing distance from the tumor border in the cancer tissue. This correlated statistically with FOXE1 scores. However, a similar pattern and correlation were not observed in the normal tissue, suggesting that there is no direct link of FOXE1 overexpression with cell proliferation *per se*. To address stromal effects, we assessed the distribution of tumor-associated macrophages that are known to be important regulators of the cancer microenvironment (41). CD68 immunostaining demonstrated preferential accumulation of macrophages around the tumor border, either on the side of the tumor or the normal tissue, but large interspecimen variations were observed; CD68 staining did not correlate with any FOXE1 scores in either tumor or normal tissue (A.B., unpublished data). The effect of reactive oxygen species was examined using an antibody to 4-HNE, a marker of peroxide-induced damage (42). Immunostaining showed antigen localization in the cytoplasm of normal thyroid cells, while cancer tissue was predominantly negative, probably due to the downregulation of thyroid peroxidase in PTC; also, no gradient staining was observed (A.B., unpublished data). Thus, neither of these biological processes could explain the four zone FOXE1 expression pattern. Further experiments employing gene expression microarray analysis of cells microdissected from the four regions may provide insights into the differential expression of FOXE1 and the underlying mechanisms.

Intracellular localization of FOXE1 appeared to be markedly different in cancer and normal epithelium. In our series, nuclear FOXE1 staining was intense to moderate with weak

Table 2. Clinical and Pathological Parameters According to the Nuclear FOXE1 Expression in the T Close and N Close Zones

	Tumor			*Normal thyroid*		
	< Median, n = *24*	*≥ Median,* n = *24*	p *value*[a]	*< Median,* n = *24*	*≥ Median,* n = *24*	p-*value*[a]
Baseline characteristics						
Age, mean ± SD (range), years	58.0 ± 11.1 (41–76)	59.5 ± 8.2 (40–72)	0.64	56.8 ± 9.8 (40–76)	60.4 ± 9.4 (44–75)	0.19
Sex			0.33			1.00
Male	4	1		3	2	
Female	20	23		21	22	
Cancer characteristics						
pT (1 + 2 vs. 3 + 4) category[b]			0.77			0.15
1	7	12		10	9	
2	5	2		6	1	
3	10	10		6	14	
4	2	0		2	0	
N category[b]			0.08			0.56
0	7	14		9	12	
1	17	10		15	12	
M1 category[b]	0	0	NC	0	0	NC
Clinical stage (I + II vs. III + IV)			0.77			0.77
I	6	9		8	7	
II	2	1		2	1	
III	14	14		12	16	
IV	2	0		2	0	
Tumor size, mean ± SD (range), mm	21.0 ± 9.6	16.8 ± 7.0	0.37	21.2 ± 9.1	16.9 ± 7.7	0.12
≤ 10 mm	3	5		2	6	
11–20 mm	13	15		15	13	
> 20 mm	8	4		7	5	
Tumor capsule (full/partial)	4	8	0.31	6	6	1.00
Capsular invasion	2	6	0.24	4	4	1.00
Histopathological variant			0.34			0.48
Papillary	14	14		12	16	
Follicular	1	4		3	2	
Other[c]	9	6		9	6	
Oxyphilic changes[d]	10	8	0.77	7	11	0.37
Tumor multifocality	2	5	0.42	3	4	1.00
Intrathyroidal spread	14	12	0.84	13	13	1.00
Extrathyroidal extension	11	9	0.77	7	13	0.14
Vascular invasion	12	7	0.66	12	7	0.24
Intratumoral lymphocytic infiltration	6	5	1.00	9	2	0.04
Peritumoral lymphocytic infiltration	19	17	0.74	19	17	0.74
Tumor fibrosis[e]	13	18	0.23	17	14	0.55
Concomitant thyroid disease[f]	6	10	0.36	5	11	0.12
MCM2 expression in cancer tissue						
MCM2 close	26.5 ± 12.1	32.6 ± 14.6	0.14	29.2 ± 15.5	30.1 ± 13.5	0.91
MCM2 distant	16.6 ± 9.5	23.8 ± 13.0	0.03	17.4 ± 13.9	23.4 ± 10.0	0.04
Genetic data[g]						
rs955513 (G/G vs. G/A + A/A)	21/2	22/2	1.00	23/1	20/3	0.35
rs1867277 (G/G vs. G/A + A/A)	19/4	14/9	0.19	17/7	16/6	1.00

[a]Two-tailed values based on Mann-Whitney test for continuous variables and Fisher's exact test or its extension for categorical variables. NC, not calculated.

[b]pT (pathologically assessed primary tumor size and extension), N (regional lymph node involvement), and M (distant metastasis) categories are defined according to UICC TNM classification (26).

[c]Solid variant, oxyphilic variant and tumors with mixed growth pattern.

[d]Includes focal oxyphilic changes and oxyphilic tumors.

[e]Only moderate/extensive fibrosis.

[f]Includes solitary hyperplastic nodules, multinodular goiter, chronic lymphocytic thyroiditis, Hashimoto's thyroiditis, and follicular adenomas.

[g]rs955513 and rs1867277 were successfully genotyped in 47 and 46 cases, respectively.

Table 3. Factors Associating with Nuclear FOXE1 Expression in the T Close Zone

Factor	*Comparison*	*Odds ratio*	*95% CI*	p *value*[a]
Multifocality	Absent vs. present	16.11	[1.28–203.43]	0.032
rs1867277	G/G vs. G/A+A/A[b]	7.02	[1.12–43.84]	0.037
Capsular invasion	Absent vs. present	10.44	[0.98–110.70]	0.051
Nodal disease	Absent vs. present	0.23	[0.05–1.13]	0.230

[a]Based on the likelihood ratio test.
[b]The dominant model, which compares individuals homozygous for the major allele (G/G) with the combined subgroup of hetero- or homozygous carriers of the risk allele (i.e., G/A or A/A) was used.
CI, confidence interval.

cytoplasmic signal in the normal thyroid, which is in agreement with an earlier report (15). PTC tissues exhibited an evident cytoplasmic overexpression and a decreased accumulation in the nucleus. Loss of nuclear FOXE1 expression in thyroid tumors has been proposed to be associated with tumor dedifferentiation and is most pronounced in anaplastic thyroid carcinomas, which are virtually devoid of FOXE1 (24,25).

The aberrant cytoplasmic FOXE1 expression in PTC cells may be suggestive of its relationship to cancer biology. For example, a forkhead-box domain-containing transcription factor FOXP1 shows loss of nuclear expression with more frequent cytoplasmic accumulation in endometrial carcinomas compared with normal endometrium (43). The aberrant cytoplasmic localization of β-catenin has prognostic significance in thyroid papillary microcarcinoma and other cancers (44,45). However, we do not propose that FOXE1 might be used for PTC prognostication because all tumors in our series, regardless of their size or stage, displayed protein translocation to the cytoplasm. The mechanism of FOXE1 accumulation in the cytoplasm has not been studied so far. It is tempting to speculate that one or several signaling cascades might result in FOXE1 modification causing its stabilization and export to or retention in the cytoplasm. For example, this may be due in part to the SHH/GLI and WNT pathways both of which regulate *FOXE1* expression (16,46–48) and are active in PTC (49,50). The MAP kinase cascade, whose functional importance in the pathogenesis of PTC is apparent based on oncogenic mutations at several steps, would be an unlikely candidate since phospho-ERK1/2 expression observed through immunohistochemistry has been reported to be irregular and did not follow an ordered spatial distribution (51–55). Further functional studies are necessary to clarify whether FOXE1 translocation to the cytoplasm is an active contributor to PTC or a consequence of cell transformation.

We also made an attempt to link FOXE1 expression with the results of genetic association studies, which pointed to *FOXE1* as a genetic determinant of thyroid cancer. Two SNPs, the rs965513 located upstream of *FOXE1* and rs1867277 in the 5'UTR of the gene, are strongly associated with the risk of PTC. It is worth noting that rs965513 is the strongest genetic marker of thyroid cancer (principally of PTC) in both (adult) sporadic (5,8,9) and (mostly childhood and adolescent) radiation-induced PTC (6). Activated oncogenes underlying PTC in adult and young patients are generally distinct and include point mutations (*BRAF*, *RAS* family) or gene rearrangements (*RET/PTC*, *TRK*), respectively (4). Therefore, the role of FOXE1 in thyroid carcinogenesis would be rather more universal and independent of the type of oncogenic drive.

According to our analysis, the presence of risk allele (A) in rs1867277 was associated with higher nuclear expression of FOXE1 in cancer cells at the tumor border. It has been demonstrated that rs1867277 (A) is responsible for increased FOXE1 expression through the recruitment of the USF1/USF2 transcription factors (7). Although there have been no studies specifically focusing on USF1 and/or USF2 expression in PTC, data from microarrays suggest that the mRNA levels of these transcription factors are not decreased in cancer tissue as compared to the normal thyroid (https://www.oncomine.org/resource/main.html#v:15). USF1 and USF2 transcripts are also detectable in the rat thyroid cell line FRTL-5 (56). Taking these reports together with our results, one may suggest that transcriptional regulation of the *FOXE1* gene by USF1/USF2 may be functional in PTC.

Interestingly, rs1867277 was recently reported to be in strong linkage disequilibrium with the *FOXE1* region encoding the polyalanine stretch of the protein in Caucasian individuals (10). Risk allele (rs1867277, A) corresponds to the 16 alanine repeat–bearing FOXE1, whose transcriptional activity is modestly different from that of the major 14 alanine isoform. It has also been claimed that *FOXE1* mRNA was expressed more abundantly in thyroid biopsies from PTC patients homozygous for the 16 alanine allele than in patients homozygous for the 14 alanine genotype (57). While there are no data on the relationship between the number of alanine repeats and protein stability, the higher *FOXE1* mRNA expression level, presumably due to both USF1/USF2 recruitment, and the higher conformational stability, might result in FOXE1 overexpression. This could explain, at least in part, the association between elevated FOXE1 levels and rs1867277, which we observed in our PTC series. Such a hypothesis should, however, be considered cautiously because the linkage disequilibrium block structure may be different in individuals of European and Japanese ancestry.

In summary, our study demonstrates that while nuclear FOXE1 is generally decreased in PTC, its local overexpression at the tumor edge might be of significance. Besides the detected genotype–phenotype correlation, indicators of tumor aggressiveness such as multifocality and (marginally) capsular invasion also appeared to be associated with nuclear FOXE1 accumulation in cancer epithelial cells in the vicinity of the tumor border. In addition, no principal difference in FOXE1 expression was seen between microcarcinomas and PTCs of larger size. The most plausible interpretation integrating these findings would be that FOXE1 plays a role at the

tumor–host interface and facilitates carcinogenesis beginning from the early stage of tumor development. Functional studies are warranted to clarify the exact mechanism of FOXE1 action.

Acknowledgments

This work was supported in part by research grants 22390189 and 24591369 from the Japan Society for the Promotion of Science (JSPS).

Disclosure Statement

No competing financial interests exist.

References

1. Siegel R, Naishadham D, Jemal A 2012 Cancer statistics, 2012. CA Cancer J Clin **62:**10–29.
2. Center for Cancer Control and Information Services NCC, Japan. Cancer Statistics in Japan. http://ganjoho.jp/pro/statistics/en/table_download.html (accessed September 27, 2012).
3. DeLellis RA 2006 Pathology and genetics of thyroid carcinoma. J Surg Oncol **94:**662–669.
4. Nikiforov YE 2011 Molecular analysis of thyroid tumors. Mod Pathol 24**(Suppl 2):**S34–43.
5. Gudmundsson J, Sulem P, Gudbjartsson DF, Jonasson JG, Sigurdsson A, Bergthorsson JT, He H, Blondal T, Geller F, Jakobsdottir M, Magnusdottir DN, Matthiasdottir S, Stacey SN, Skarphedinsson OB, Helgadottir H, Li W, Nagy R, Aguillo E, Faure E, Prats E, Saez B, Martinez M, Eyjolfsson GI, Bjornsdottir US, Holm H, Kristjansson K, Frigge ML, Kristvinsson H, Gulcher JR, Jonsson T, Rafnar T, Hjartarsson H, Mayordomo JI, de la Chapelle A, Hrafnkelsson J, Thorsteinsdottir U, Kong A, Stefansson K 2009 Common variants on 9q22.33 and 14q13.3 predispose to thyroid cancer in European populations. Nat Genet **41:**460–464.
6. Takahashi M, Saenko VA, Rogounovitch TI, Kawaguchi T, Drozd VM, Takigawa-Imamura H, Akulevich NM, Ratanajaraya C, Mitsutake N, Takamura N, Danilova LI, Lushchik ML, Demidchik YE, Heath S, Yamada R, Lathrop M, Matsuda F, Yamashita S 2010 The FOXE1 locus is a major genetic determinant for radiation-related thyroid carcinoma in Chernobyl. Hum Mol Genet **19:**2516–2523.
7. Landa I, Ruiz-Llorente S, Montero-Conde C, Inglada-Perez L, Schiavi F, Leskela S, Pita G, Milne R, Maravall J, Ramos I, Andia V, Rodriguez-Poyo P, Jara-Albarran A, Meoro A, del Peso C, Arribas L, Iglesias P, Caballero J, Serrano J, Pico A, Pomares F, Gimenez G, Lopez-Mondejar P, Castello R, Merante-Boschin I, Pelizzo MR, Mauricio D, Opocher G, Rodriguez-Antona C, Gonzalez-Neira A, Matias-Guiu X, Santisteban P, Robledo M 2009 The variant rs1867277 in FOXE1 gene confers thyroid cancer susceptibility through the recruitment of USF1/USF2 transcription factors. PLoS Genet **5:**e1000637.
8. Matsuse M, Takahashi M, Mitsutake N, Nishihara E, Hirokawa M, Kawaguchi T, Rogounovitch T, Saenko V, Bychkov A, Suzuki K, Matsuo K, Tajima K, Miyauchi A, Yamada R, Matsuda F, Yamashita S 2011 The FOXE1 and NKX2-1 loci are associated with susceptibility to papillary thyroid carcinoma in the Japanese population. J Med Genet **48:**645–648.
9. Jones AM, Howarth KM, Martin L, Gorman M, Mihai R, Moss L, Auton A, Lemon C, Mehanna H, Mohan H, Clarke SE, Wadsley J, Macias E, Coatesworth A, Beasley M, Roques T, Martin C, Ryan P, Gerrard G, Power D, Bremmer C, Tomlinson I, Carvajal-Carmona LG 2012 Thyroid cancer susceptibility polymorphisms: confirmation of loci on chromosomes 9q22 and 14q13, validation of a recessive 8q24 locus and failure to replicate a locus on 5q24. J Med Genet **49:**158–163.
10. Bullock M, Duncan EL, O'Neill C, Tacon L, Sywak M, Sidhu S, Delbridge L, Learoyd D, Robinson BG, Ludgate M, Clifton-Bligh RJ 2012 Association of FOXE1 polyalanine repeat region with papillary thyroid cancer. J Clin Endocrinol Metab **97:**E1814–1819.
11. Chadwick BP, Obermayr F, Frischauf AM 1997 FKHL15, a new human member of the forkhead gene family located on chromosome 9q22. Genomics **41:**390–396.
12. Zannini M, Avantaggiato V, Biffali E, Arnone MI, Sato K, Pischetola M, Taylor BA, Phillips SJ, Simeone A, Di Lauro R 1997 TTF-2, a new forkhead protein, shows a temporal expression in the developing thyroid which is consistent with a role in controlling the onset of differentiation. EMBO J **16:**3185–3197.
13. Trueba SS, Auge J, Mattei G, Etchevers H, Martinovic J, Czernichow P, Vekemans M, Polak M, Attie-Bitach T 2005 PAX8, TITF1, and FOXE1 gene expression patterns during human development: new insights into human thyroid development and thyroid dysgenesis-associated malformations. J Clin Endocrinol Metab **90:**455–462.
14. Clifton-Bligh RJ, Wentworth JM, Heinz P, Crisp MS, John R, Lazarus JH, Ludgate M, Chatterjee VK 1998 Mutation of the gene encoding human TTF-2 associated with thyroid agenesis, cleft palate and choanal atresia. Nat Genet **19:**399–401.
15. Sequeira M, Al-Khafaji F, Park S, Lewis MD, Wheeler MH, Chatterjee VK, Jasani B, Ludgate M 2003 Production and application of polyclonal antibody to human thyroid transcription factor 2 reveals thyroid transcription factor 2 protein expression in adult thyroid and hair follicles and prepubertal testis. Thyroid **13:**927–932.
16. Eichberger T, Regl G, Ikram MS, Neill GW, Philpott MP, Aberger F, Frischauf AM 2004 FOXE1, a new transcriptional target of GLI2 is expressed in human epidermis and basal cell carcinoma. J Invest Dermatol **122:**1180–1187.
17. Venza I, Visalli M, Tripodo B, De Grazia G, Loddo S, Teti D, Venza M 2010 FOXE1 is a target for aberrant methylation in cutaneous squamous cell carcinoma. Br J Dermatol **162:**1093–1097.
18. Park E, Gong EY, Romanelli MG, Lee K 2012 Suppression of estrogen receptor-alpha transactivation by thyroid transcription factor-2 in breast cancer cells. Biochem Biophys Res Commun **421:**532–537.
19. Sato N, Fukushima N, Maitra A, Matsubayashi H, Yeo CJ, Cameron JL, Hruban RH, Goggins M 2003 Discovery of novel targets for aberrant methylation in pancreatic carcinoma using high-throughput microarrays. Cancer Res **63:**3735–3742.
20. Aza-Blanc P, Di Lauro R, Santisteban P 1993 Identification of a cis-regulatory element and a thyroid-specific nuclear factor mediating the hormonal regulation of rat thyroid peroxidase promoter activity. Mol Endocrinol **7:**1297–1306.
21. Civitareale D, Saiardi A, Falasca P 1994 Purification and characterization of thyroid transcription factor 2. Biochem J **304(Pt 3):**981–985.
22. Ortiz L, Zannini M, Di Lauro R, Santisteban P 1997 Transcriptional control of the forkhead thyroid transcription factor TTF-2 by thyrotropin, insulin, and insulin-like growth factor I. J Biol Chem **272:**23334–23339.

23. Sequeira MJ, Morgan JM, Fuhrer D, Wheeler MH, Jasani B, Ludgate M 2001 Thyroid transcription factor-2 gene expression in benign and malignant thyroid lesions. Thyroid **11:**995–1001.
24. Nonaka D, Tang Y, Chiriboga L, Rivera M, Ghossein R 2008 Diagnostic utility of thyroid transcription factors Pax8 and TTF-2 (FoxE1) in thyroid epithelial neoplasms. Mod Pathol **21:**192–200.
25. Zhang P, Zuo H, Nakamura Y, Nakamura M, Wakasa T, Kakudo K 2006 Immunohistochemical analysis of thyroid-specific transcription factors in thyroid tumors. Pathol Int **56:**240–245.
26. Sobin LH, Gospodarowicz MK, Wittekind C 2009 TNM classification of malignant tumours. 7th ed. Wiley-Blackwell, Oxford, UK.
27. DeLellis RA 2004 Pathology and genetics of tumours of endocrine organs. IARC Press, Lyon.
28. King J, Thatcher N, Pickering C, Hasleton P 2006 Sensitivity and specificity of immunohistochemical antibodies used to distinguish between benign and malignant pleural disease: a systematic review of published reports. Histopathology **49:**561–568.
29. Hanna-Morris A, Badvie S, Cohen P, McCullough T, Andreyev HJ, Allen-Mersh TG 2009 Minichromosome maintenance protein 2 (MCM2) is a stronger discriminator of increased proliferation in mucosa adjacent to colorectal cancer than Ki-67. J Clin Pathol **62:**325–330.
30. Cho Mar K, Eimoto T, Nagaya S, Tateyama H 2006 Cell proliferation marker MCM2, but not Ki67, is helpful for distinguishing between minimally invasive follicular carcinoma and follicular adenoma of the thyroid. Histopathology **48:**801–807.
31. Mehrotra P, Gonzalez MA, Johnson SJ, Coleman N, Wilson JA, Davies BR, Lennard TW 2006 Mcm-2 and Ki-67 have limited potential in preoperative diagnosis of thyroid malignancy. Laryngoscope **116:**1434–1438.
32. Brabletz T, Jung A, Hermann K, Gunther K, Hohenberger W, Kirchner T 1998 Nuclear overexpression of the oncoprotein beta-catenin in colorectal cancer is localized predominantly at the invasion front. Pathol Res Pract **194:** 701–704.
33. El-Gendi S, Al-Gendi A 2011 Assessment of tumor budding in colorectal carcinoma: correlation with beta-catenin nuclear expression. J Egypt Natl Canc Inst **23:**1–9.
34. Jabs WJ, Busse M, Kruger S, Jocham D, Steinhoff J, Doehn C 2005 Expression of C-reactive protein by renal cell carcinomas and unaffected surrounding renal tissue. Kidney Int **68:**2103–2110.
35. Hong SW, Kang YK, Lee B, Lee WY, Jang YG, Paik IW, Lee H 2011 Matrix metalloproteinase-2 and -7 expression in colorectal cancer. J Korean Soc Coloproctol **27:**133–139.
36. Johansson M, Brannstrom T, Bergenheim AT, Henriksson R 2002 Spatial expression of VEGF-A in human glioma. J Neurooncol **59:**1–6.
37. Scarpino S, Stoppacciaro A, Ballerini F, Marchesi M, Prat M, Stella MC, Sozzani S, Allavena P, Mantovani A, Ruco LP 2000 Papillary carcinoma of the thyroid: hepatocyte growth factor (HGF) stimulates tumor cells to release chemokines active in recruiting dendritic cells. Am J Pathol **156:**831–837.
38. Ugolini C, Basolo F, Proietti A, Vitti P, Elisei R, Miccoli P, Toniolo A 2007 Lymphocyte and immature dendritic cell infiltrates in differentiated, poorly differentiated, and undifferentiated thyroid carcinoma. Thyroid **17:**389–393.
39. Proietti A, Ugolini C, Melillo RM, Crisman G, Elisei R, Santoro M, Minuto M, Vitti P, Miccoli P, Basolo F 2011 Higher intratumoral expression of CD1a, tryptase, and CD68 in a follicular variant of papillary thyroid carcinoma compared to adenomas: correlation with clinical and pathological parameters. Thyroid **21:**1209–1215.
40. Kojc N, Zidar N, Vodopivec B, Gale N 2005 Expression of CD34, alpha-smooth muscle actin, and transforming growth factor beta1 in squamous intraepithelial lesions and squamous cell carcinoma of the larynx and hypopharynx. Hum Pathol **36:**16–21.
41. Qian BZ, Pollard JW 2010 Macrophage diversity enhances tumor progression and metastasis. Cell **141:**39–51.
42. Tanaka T, Nishiyama Y, Okada K, Hirota K, Matsui M, Yodoi J, Hiai H, Toyokuni S 1997 Induction and nuclear translocation of thioredoxin by oxidative damage in the mouse kidney: independence of tubular necrosis and sulfhydryl depletion. Lab Invest **77:**145–155.
43. Giatromanolaki A, Koukourakis MI, Sivridis E, Gatter KC, Harris AL, Banham AH 2006 Loss of expression and nuclear/cytoplasmic localization of the FOXP1 forkhead transcription factor are common events in early endometrial cancer: relationship with estrogen receptors and HIF-1alpha expression. Mod Pathol **19:**9–16.
44. Lantsov D, Meirmanov S, Nakashima M, Kondo H, Saenko V, Naruke Y, Namba H, Ito M, Abrosimov A, Lushnikov E, Sekine I, Yamashita S 2005 Cyclin D1 overexpression in thyroid papillary microcarcinoma: its association with tumour size and aberrant beta-catenin expression. Histopathology **47:**248–256.
45. Cheuk W, Chan JK 2004 Subcellular localization of immunohistochemical signals: knowledge of the ultrastructural or biologic features of the antigens helps predict the signal localization and proper interpretation of immunostains. Int J Surg Pathol **12:**185–206.
46. Brancaccio A, Minichiello A, Grachtchouk M, Antonini D, Sheng H, Parlato R, Dathan N, Dlugosz AA, Missero C 2004 Requirement of the forkhead gene Foxe1, a target of sonic hedgehog signaling, in hair follicle morphogenesis. Hum Mol Genet **13:**2595–2606.
47. Venza I, Visalli M, Parrillo L, De Felice M, Teti D, Venza M 2011 MSX1 and TGF-beta3 are novel target genes functionally regulated by FOXE1. Hum Mol Genet **20:**1016–1025.
48. Choi JH, Kim BK, Kim JK, Lee HY, Park JK, Yoon SK 2011 Downregulation of Foxe1 by HR suppresses Msx1 expression in the hair follicles of Hr(Hp) mice. BMB Rep **44:**478–483.
49. Xu X, Ding H, Rao G, Arora S, Saclarides CP, Esparaz J, Gattuso P, Solorzano CC, Prinz RA 2012 Activation of the Sonic Hedgehog pathway in thyroid neoplasms and its potential role in tumor cell proliferation. Endocr Relat Cancer **19:**167–179.
50. Sastre-Perona A, Santisteban P 2012 Role of the wnt pathway in thyroid cancer. Front Endocrinol (Lausanne) **3:**31.
51. Baba K, Ishibashi M, Kaida H, Fujii T, Hiromatsu Y, Kawahara A, Kage M, Hayabuchi N 2011 Relation between (99m)Tc-tetrofosmin thyroid scintigraphy and mitogen-activated protein kinase in papillary thyroid cancer patients. Jpn J Radiol **29:**533–539.
52. Kang DY, Kim KH, Kim JM, Kim SH, Kim JY, Baik HW, Kim YS 2007 High prevalence of RET, RAS, and ERK expression in Hashimoto's thyroiditis and in papillary thyroid carcinoma in the Korean population. Thyroid **17:**1031–1038.

53. Mitsiades CS, Negri J, McMullan C, McMillin DW, Sozopoulos E, Fanourakis G, Voutsinas G, Tseleni-Balafouta S, Poulaki V, Batt D, Mitsiades N 2007 Targeting BRAFV600E in thyroid carcinoma: therapeutic implications. Mol Cancer Ther **6:**1070–1078.
54. Zuo H, Nakamura Y, Yasuoka H, Zhang P, Nakamura M, Mori I, Miyauchi A, Kakudo K 2007 Lack of association between BRAF V600E mutation and mitogen-activated protein kinase activation in papillary thyroid carcinoma. Pathol Int **57:**12–20.
55. Shin E, Hong SW, Kim SH, Yang WI 2004 Expression of down stream molecules of RET (p-ERK, p-p38 MAPK, p-JNK and p-AKT) in papillary thyroid carcinomas. Yonsei Med J **45:**306–313.
56. Jung HS, Kim KS, Chung YJ, Chung HK, Min YK, Lee MS, Lee MK, Kim KW, Chung JH 2007 USF inhibits cell proliferation through delay in G2/M phase in FRTL-5 cells. Endocr J **54:**275–285.
57. Kallel R, Belguith-Maalej S, Akdi A, Mnif M, Charfeddine I, Galofre P, Ghorbel A, Abid M, Marcos R, Ayadi H, Velazquez A, Hadj Kacem H 2010 Genetic investigation of FOXE1 polyalanine tract in thyroid diseases: new insight on the role of FOXE1 in thyroid carcinoma. Cancer Biomark **8:**43–51.

Address correspondence to:
Vladimir Saenko, PhD
Department of Health Risk Control
Nagasaki University Graduate School of Biomedical Sciences
1-12-4 Sakamoto
Nagasaki 852-8523
Japan

E-mail: saenko@nagasaki-u.ac.jp